

## DEVELOPMENT, CHARACTERIZATION AND ANTIBACTERIAL PROPERTIES OF SILVER NANOPARTICLES LOADED SODIUM ALGINATE/XANTHAN GUM MICROBEADS FOR DRUG DELIVERY APPLICATIONS

E. VENKATA RAMANA, NASEEM\*

Department of Pharmaceutical Chemistry, Telangana University, Nizamabad, Telangana 503322, India

\*Email: naseemprof@gmail.com

Received: 08 Dec 2022, Revised and Accepted: 17 Mar 2023

### ABSTRACT

**Objective:** The aim of this study is to create pH-responsive drug carriers, which are useful because they have the potential to improve treatment efficacy by controlling the release rate of ofloxacin from the polymer matrix.

**Methods:** In the first step, silver nanoparticles (Ag NPs) were synthesized from silver nitrate using leaf extract of *phyllanthus urinaria* L as a reducing agent. In the second step, Ag-NPs-loaded polymeric microbeads were synthesized using sodium alginate (SA) and xanthan gum (XG) for controlled release of ofloxacin (OFLX). The developed microbeads were characterized by Fourier transform infrared spectroscopy (FTIR), X-ray diffraction (XRD), transition electron microscopy (TEM), Selected Area Electron Diffraction (SAED), and scanning electron microscopy (SEM). Swelling and *in vitro* release studies were performed at pH 2.0 and 7.4 at 37 °C. The *in vitro* antibacterial activity of microbeads were tested against *S. mutans*, *K. pneumoniae*, and *B. subtilis*. The release kinetics and mechanism were analyzed by fitting the release data into different kinetic models and the korsmeyer-peppas equation.

**Results:** FTIR confirms the generation of silver nanoparticle and also the generation of polymeric microbeads. SEM studies reveal the developed microbeads are spherical in shape with rough surfaces. TEM studies reveal the size of 20-40 nm. XRD analysis reveals the molecular dispersion of DOX and the presence of silver nanoparticles in the polymeric matrix. Investigations of *in vitro* release and swelling studies show that the developed microbeads are relatively suitable for intestinal drug delivery because higher release rate was observed at pH 7.4. The developed microbead follows non-Fickian diffusion drug release mechanism. The created samples exhibited antimicrobial activity against *S. mutans*, *K. pneumoniae*, and *B. subtilis*.

**Conclusion:** The results indicate that microbeads containing OFLX and silver nanoparticles are effective drug-delivery vehicles. A further warrant is required for the use of manufactured microbeads in drug delivery applications.

**Keywords:** Sodium alginate, Xanthan gum, Silver nanoparticles, Microbeads, Ofloxacin, Antibacterial activity

© 2023 The Authors. Published by Innovare Academic Sciences Pvt Ltd. This is an open access article under the CC BY license (<https://creativecommons.org/licenses/by/4.0/>)  
DOI: <https://dx.doi.org/10.22159/ijap.2023v15i3.47028>. Journal homepage: <https://innovareacademics.in/journals/index.php/ijap>

### INTRODUCTION

Nanotechnology is the world's fastest-growing industrial sector, and there is a frenetic hunt for novel nanomaterials and processes to manufacture nanoparticles [1, 2]. Nanomedicine, a new field that has grown out of the combination of nanotechnology and medicine, is one area where nanotechnology is used in a lot of different ways. Nanotechnology can enhance our understanding of living cells and their interactions at the molecular level. Several nanoparticle-based treatments for infections, vaccinations, and kidney disorders have been approved for clinical use [3, 4]. There are numerous ways to create nanoparticles, including chemical, physical, and biological methods. When compared to other possible platforms, plants offer a safer environment for nanoparticle production due to the absence of harmful chemicals and also the presence of natural capping agents [5-7].

Silver nanoparticles are frequently used in catalysis, chemical sensing, biosensing, photonics, electronics, and medicines due to their unique features [8-10]. Nanoparticles of silver show significant promise for use in biological applications, including antibacterial activity [11, 12]. The antimicrobial properties of silver nanoparticles make them suitable for usage in a variety of consumer goods, including fabrics, food storage units, home appliances, and medical devices [13]. Silver is a potent antibacterial substance with low toxicity [14]. The most significant application of silver and silver nanoparticles is in the medical sector, such as in tropical ointments used to prevent infection in burns and open wounds [15]. In recent years, silver nanoparticles have become one of the most widely studied nanoparticles. Nanoscale silver particles typically range in size from 1 to 100 nm. Because they have a high surface area-to-volume ratio, silver nanoparticles are able to kill microbes effectively at extremely low concentrations. Moreover, they are inexpensive and have demonstrated little cytotoxicity and immunogenicity. In light of this, silver nanoparticles may be used in a wide variety of medical applications [16].

Polymers have played a crucial role in the development of drug delivery technology by enabling the controlled release of bioactive molecules in constant doses over extended periods, cyclic dosage, and constant release of both hydrophilic and hydrophobic drugs. The primary roles of polymers are to protect the drug from its physiological environment and to prolong its release to improve its stability [17, 18]. Sodium alginate is one of the natural biodegradable polymers extracted from brown algae [19-21]. SA microbeads are one of the multiparticulate drug delivery systems that have been developed to achieve extended or controlled drug delivery, increase bioavailability or stability, and target drugs to specific areas [22-24]. Another polymer, xanthan gum, is a natural polymer obtained from *Xanthomonas campestris* [25]. XG has important economic and pharmaceutical benefits because of its controlled release rate, superior drug retarding capacity, and absence of an initial burst release [26]. According to Kar *et al.* [27] xanthan gum has a sustained drug release pattern that reduces dose frequency. Tao *et al.* [28] said that chemical crosslinking with xanthan gum makes hydrogels that are more flexible, more swollen in nature, and sustained the release of bioactive agents.

In this study, we used the gelation method to create pH-responsive polymeric microbeads with sodium alginate and xanthan gum for the controlled release of OFLX. The microbeads are embedded with silver nanoparticles, and their antibacterial activity was investigated. In addition, we conducted *in vitro* release and swelling studies, and the results are discussed in this paper.

### MATERIALS AND METHODS

#### Materials

XG and NaOH are purchased from Sigma Aldrich (St. Louis, MO, USA). SA, Silver nitrate and calcium chloride were purchased from Sd. Fine chemicals, Mumbai, India. OFLX purchased from Sisco Research

Laboratories Pvt. Ltd. Mumbai, India. Double distilled water was used throughout the experiment.

### Preparation of silver nanoparticles

The fresh leaf of *Phyllanthus urinaria* L (Girraj Government College (A), Telangana Hyderabad; Herbarium with voucher specimen No.50210) broth solution was prepared by taking 10 gms of *P. urinaria* L dried leaves in a 250 ml Erlenmeyer flask containing 100 ml of double distilled water and boiled for 30 min at 60 °C. After cooling, the extract was filtered using Whatman No.1 filter paper and stored at 4 °C for further use. The filtrate was transferred to a 250 ml beaker containing 100 ml of AgNO<sub>3</sub> (1 mmol) solution and exposed to sunlight for half an hour. After the addition of leaf extract, the color changes from colorless to brownish-yellow, indicating the generation of nanoparticles. The solution was then centrifuged at 15,000 rpm for 10 min, and the nanoparticles were collected, washed with ethanol several times, and stored in airtight containers for further usage. In this reaction, leaf extract acts as a reducing agent, and the stabilized solution leads to the formation of nanoparticles.

### Development of polymeric microbeads

OFLX-loaded microbeads were fabricated using an ionotropic gelation technique. Briefly, 200 mg of SA and 200 mg of XG were dissolved in 10 ml of water separately. After that, combine the SA and XG solutions and stir for 6 h. To this mixture, add 100 mg of Ag NPs and 100 mg of OFLX and sonicate for 10 min. Then the mixture is stirred continuously until the formation of a homogenous solution. The resulting suspension was then poured into CaCl<sub>2</sub>. Instantaneously, spherical beads were manufactured and kept for forty minutes. The obtained microbeads are named as SAXG-NPs-OFLX. The beads were taken out of the solution by decanting them, and then they were washed several times with distilled water to get rid of any leftover drug molecules. Finally, they were left at room temperature overnight to dry in the air. Similarly, the microbeads without NPs are synthesized by the above procedure. During the preparation, only OFLX was added to the polymeric solution and followed the same above procedure. The obtained microbeads are named as SAXG-OFLX.

### Characterizations techniques

FTIR spectra of OFLX, placebo, Ag NPs, SAXG-NPs-OFLX, and SAXG-OFLX microbeads were recorded between 400-4000 cm<sup>-1</sup> using model Bomem MB-3000. The X-ray diffraction of OFLX, placebo, Ag NPs, SAXG-NPs-OFLX, and SAXG-OFLX microbeads were performed by a wide-angle X-ray scattering diffractometer (Panalytical X-ray Diffractometer, model-X'pert Pro) with CuK $\alpha$  radiation ( $\lambda = 1.54060$ ) at a scanning rate of 10°/min to determine the crystallinity. The morphological characterization of microbeads was observed by using SEM (JOEL MODEL JSM 840A) with an accelerated voltage of 20 kV. Transmission electron microscopy (TEM) (JEOL JEM 2100; JEOL, Japan) was used to determine the size of developed Ag NPs.

### Antibacterial activity

The agar well diffusion method was employed to test the OFLX-loaded microbeads for their antibacterial properties. In brief, 100 ml of *S. mutans*, *K. pneumoniae*, or *B. subtilis* (obtained from MTCC, Chandigarh, India) were spread on Luria-Bertani (LB) plates. Five discs with a diameter of 6 mm were developed in the media. Aqueous solutions of test samples (SAXG-OFLX, SAXG-NPs-OFLX, Ag NPs, negative control, and positive control) were made with a concentration of 1 mg/ml, and then 100  $\mu$ l of the test sample is added to each well. Then the plates were incubated for 24 h at 37 °C. The inhibitory zones were then measured in millimetres as described in earlier reports [29].

### Encapsulation efficiency

The encapsulation efficiency (EE) of drug-loaded microbeads was determined using a formula and process described in earlier reports [30]. 10 mg of microbeads were weighed and stored overnight in 100 ml of phosphate buffer (pH 7.4, 5% absolute alcohol) at room temperature. After that, the solution is sonicated for ten minutes and then crushed to extract the drug from the microbeads. Finally, the

absorbance is measured using a UV-Visible spectrophotometer with a maximum wavelength of 287.5 nm. The percentage of encapsulation was determined using the following formula.

$$\% EE = \frac{W_2}{W_1} \times 100$$

Where W<sub>2</sub> is the total amount of OFLX in the microbeads and W<sub>1</sub> is total amount of OFLX initially added during the preparation.

### Swelling analysis

The swelling behaviour of SAXG-OFLX and SAXG-NPs-OFLX microbeads was examined using a gravimetric assay at pH 2.0 and 7.4 at 37 °C. The following equation was used to measure the percentage of swelling:

$$\% \text{ swelling degree} = \frac{W_s - W_d}{W_d} \times 100$$

Where W<sub>s</sub> is the weight of swollen beads and W<sub>d</sub> is the weight of dry beads

### In vitro drug release studies

To investigate the drug release studies of the synthesized microbeads, dissolution analysis was carried out in a dissolution tester (Model: DS 2000, Make: LabIndia, Mumbai, India). 50 mg of drug-loaded microbeads were packed in dialysis bags and placed in 500 ml of pH 2.0 and 7.4 PBS at 37 °C with 50 rpm. At regular intervals, 5 ml of dissolution media was withdrawn, analyzed using a UV spectrophotometer at 287.5 nm, and then replaced the same volume in the basket with fresh media.

### Release kinetics

The kinetics of the drug release was evaluated by integrating data into kinetic models, including zeroth, first order, Higuchi, and Korsmeyer-peppas [31, 32]. The best model was also identified based on the data fit.

## RESULTS AND DISCUSSION

### FTIR

The FTIR spectra of OFLX (a), placebo (b), SAXG-OFLX (c), Ag NPs (d), and SAXG-NPs-OFLX (e) are represented in fig. 1. The spectral peaks of OFLX are 3421 cm<sup>-1</sup> (O-H stretching frequency), 1720 cm<sup>-1</sup> (C=O stretching frequency), 1384 cm<sup>-1</sup> (COO-asymmetric stretching frequency), and 1142 cm<sup>-1</sup> (C-N stretching frequency) [33]. The spectral peaks of Ag NPs are 1599 cm<sup>-1</sup> (C=O stretching frequency), 1387 cm<sup>-1</sup> (COO-asymmetric stretching frequency), and 661 cm<sup>-1</sup> (characteristic peak of Ag NPs). The spectral peaks of placebo are 3427 cm<sup>-1</sup> (O-H stretching frequency), 1605 cm<sup>-1</sup> (C=O stretching frequency), and 1388 cm<sup>-1</sup> (COO-asymmetric stretching frequency). When the FTIR spectra of SAXG-OFLX and placebo were compared, the band that was located at 1605 cm<sup>-1</sup> in the placebo was shifted to 1599 cm<sup>-1</sup> in the SAXG-OFLX spectrum. In addition, a new peak at 1142 cm<sup>-1</sup> was identified, which may be attributed to a C-F stretching frequency. This validates that the OFLX has been loaded successfully into the polymeric matrix [30]. In the case of SAXG-NPs-OFLX, identical peaks to SAXG-OFLX were observed, as well as a peak at 728 cm<sup>-1</sup>, demonstrating that Ag NPs were successfully loaded into SAXG-NPs-OFLX.

### XRD analysis

Fig. 2 depicts the XRD patterns of OFLX, Ag NPs, placebo, SAXG-OFLX, and SAXG-NPs-OFLX. The diffraction peaks of the synthesized Ag NPs are found at 32.7°, 46.2°, 67.7°, and 76.7°, which are attributed to the (111), (200), and (220) planes. The distinctive 2 peaks of Ag NPs correspond to JCPDS No. 04-0783. Jakinala *et al.* [34] made similar observations about the synthesis of Ag NPs using insect wing extract. This demonstrates that Ag NPs are produced from AgNO<sub>3</sub>. The drug OFLX XRD pattern displays  $\emptyset$  peaks between 10° and 30°. The absence of these peaks in SAXG-OFLX and SAXG-NPs-OFLX indicates that the OFLX molecules are molecularly dispersed in the polymeric matrix. In addition, SAXG-NPs-OFLX showed peaks similar to those of Ag NPs, indicating that the Ag NPs were successfully incorporated into the polymeric matrix.

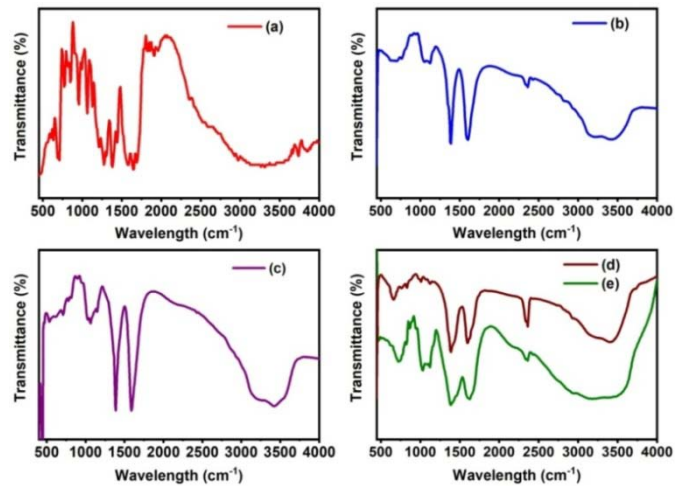


Fig. 1: FTIR spectra of (a) OFLX, (b) placebo, (c) SAXG-OFLX, (d) Ag NPs, and (e) SAXG-NPs-OFLX

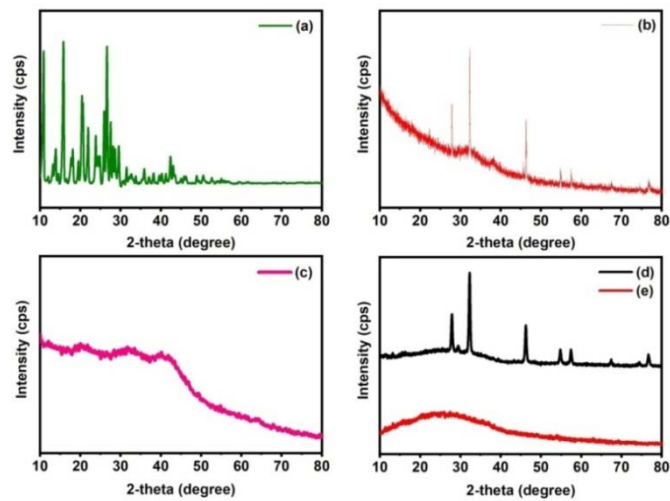


Fig. 2: XRD diffract patterns of (a) OFLX, (b) Ag NPs, (c) placebo, (d) SAXG-NPs-OFLX, and (e) SAXG-OFLX

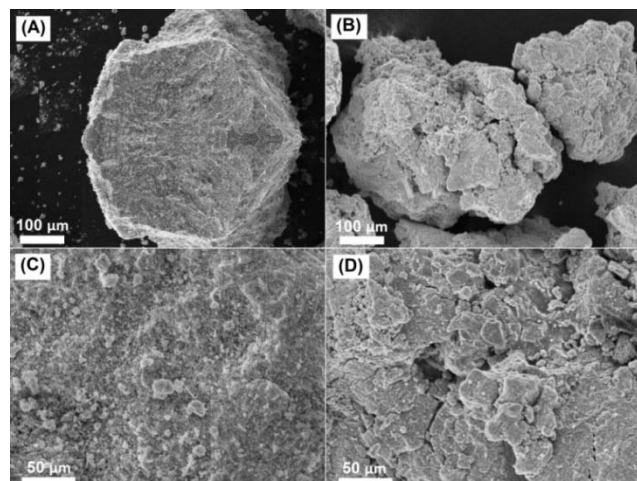


Fig. 3: SEM images of a) SAXG-OFLX and b) SAXG-NPs-OFLX microbeads. Magnification of A and B at 500x, C and D at 1000x

## SEM

The morphology of the generated microbeads was determined by SEM, and the findings are shown in fig. 3. The microbeads are semi-spherical in shape and have a rough outer surface, as depicted in fig.

3. When comparing SAXG-NPs-OFLX (fig. 3D) with SAXG-OFLX (fig. 3C), the outer surface of NPs-loaded microbeads has a more rough surface due to the incorporation of NPs. From the SEM images, it was observed that the average size of the microbeads was between 700 and 900 μm.

### R-TEM and SAED analysis

The size of Ag NPs is determined using HR-TEM analysis, and the findings are depicted in fig. 4A. According to fig. 4A, the produced Ag NPs are 20–40 nm in size. Fig. 4B displays the SAED pattern of Ag NPs, in which four distinct diffraction rings correspond to fcc Ag crystalline planes [35].

### Swelling studies

Swelling intensity is important for the controlled release of bioactive agents in polymeric drug delivery systems. In this study, swelling experiments were conducted at pH 2.0 and 7.4 at 37 °C, and the results

are displayed in fig. 5. At pH 7.4, there was more swelling than at pH 1. This may be because, at pH 7.4, the carboxylic groups in the polymeric matrix have weaker interactions with the buffer media, resulting in a more porous network that allows the entrapped drug molecules to leach out more easily. These results are in good agreement with Pallerla *et al.* [30] who found similar swelling results from their alginate-based drug delivery systems. Whereas at pH 2.0, the swelling degree was low because, at an acidic pH, the polymer matrix experiences ionic interactions with a proton of buffer medium, making the polymer matrix hydrophobic in nature, and, as a result, the swelling degree is lower. Therefore, generated microbeads are effective and promising carriers for delivering drug molecules to the intestine.

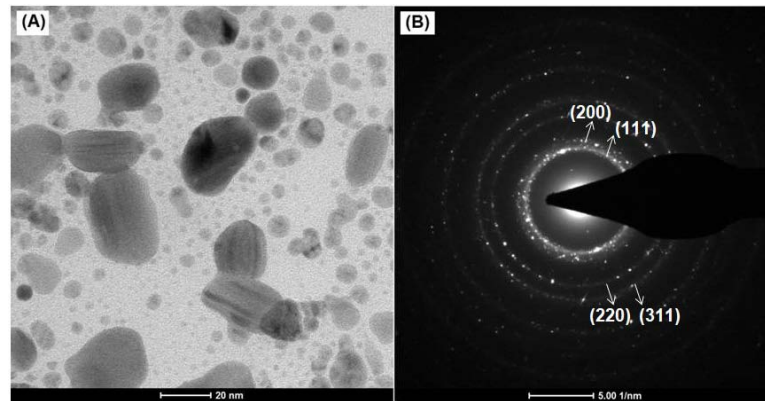


Fig. 4: TEM photograph of Ag NPs (A) and SAED pattern of Ag NPs (B). (Scale bar for A is 20 nm)

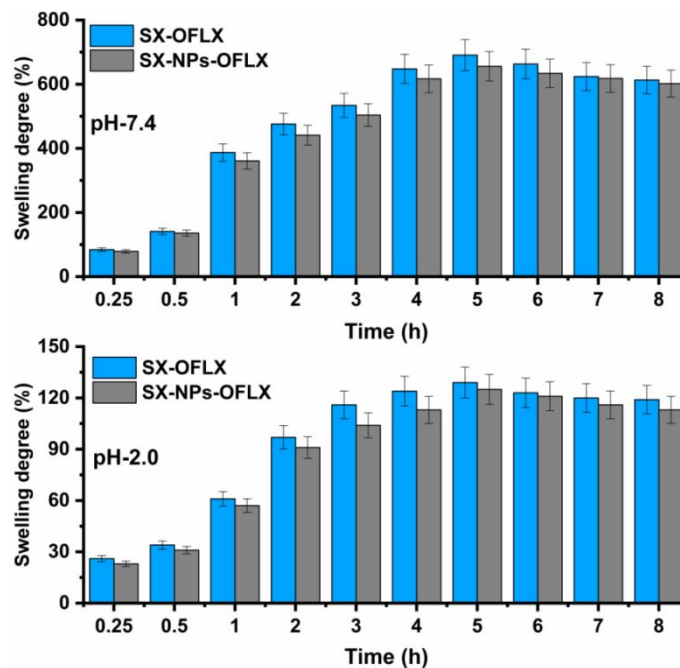


Fig. 5: Swelling studies of SAXG-OFLX and SAXG-NPs-OFLX in PBS of pH 7.4 (A) and 2.0 (B) at 37 °C (All experiments were performed triplicate, n=3)

### In vitro release studies

The EE of OFLX in SAXG-OFLX and SAXG-NPs-OFLX microbeads is 54.7% and 52.1%, respectively. The results showed that SAXG-OFLX had a higher percentage of EE than SAXG-NPs-OFLX because the polymeric network is more rigid and less swellable, leading to lower EE values. These results are in agreement with the swelling experiments previously demonstrated. The *in vitro* release tests were done in PBS at pH 2.0 and 7.4 at 37 °C and the results are

shown in fig. 6. At pH 7.4, the carboxylate group has less interaction with the buffer media. This renders the network less stiff and more porous, thus facilitating the escape of drug molecules from the polymeric matrix. At pH 2.0, the release rate was lower than at pH 7.4 because of ionic-ionic repulsions between H<sup>+</sup> ions and the polymer matrix; consequently, the polymer matrix becomes hydrophobic in nature, which inhibits the entry of solvent into the polymer matrix. Consequently, the rate of release was lowered. The release rate of SAXG-NPs-OFLX has a longer release time compared

to SAXG-OFLX; this is due to the presence of Ag NPs, which make a lonely path for OFLX migration from the polymer matrix to buffer media, hence the longer release rate. These pH-sensitive drug carriers are useful for drug delivery because they protect bioactive molecules from the acidic environment and then release them into the intestinal environment.

Table 1 shows the  $r^2$  values that were found by fitting the drug release data to different kinetic models. The release behaviour of microbeads is compatible with the first-order model as well as the Higuchi model. The mechanism of drug release involves the absorption of PBS into the polymer matrix and the diffusion of OFLX molecules from the microbeads into the surrounding environment. The rate of release is directly related to the amount of drug that is present in the system, so increasing the amount of drug will result in an increased release rate. In addition, 60% of the release data is fitted to the Korsmeyer-Peppas equation to determine the mechanism of drug profiles. The  $n$  values range from 0.295-0.608, which indicates that the microbeads diffuse in a non-Fickian manner.

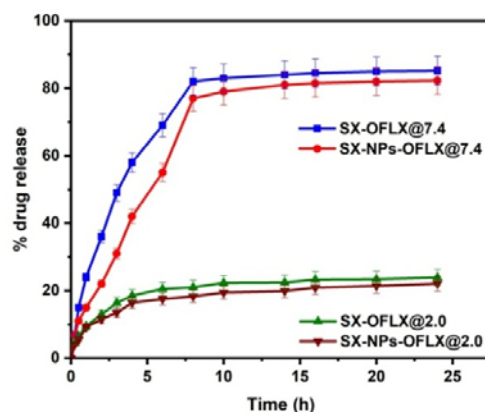


Fig. 6: *In vitro* release studies of SAXG-OFLX and SAXG-NPs-OFLX in PBS of pH 7.4 (A) and 2.0 (B) at 37 °C (All experiments were performed triplicate, n=3)

Table 1: Release kinetics parameters of SXG-OFLX and SAXG-NPs-OFLX in PBS of pH 2.0 and 7.4 at 37 °C

Code	pH	Zero-order		First order		Higuchi		Korsmeyer-Peppas	
		$K_0$	$r^2$	$K_1$	$r^2$	$K_H$	$r^2$	$n$	$r^2$
SAXG-OFLX	7.4	5.220	0.545	0.198	0.930	22.098	0.926	0.546	0.983
	2	1.450	0.744	0.018	0.836	6.244	0.817	0.382	0.966
SAXG-NPs-OFLX	7.4	4.894	0.494	0.133	0.950	20.196	0.948	0.756	0.985
	2	1.302	0.579	0.015	0.867	5.569	0.941	0.371	0.961

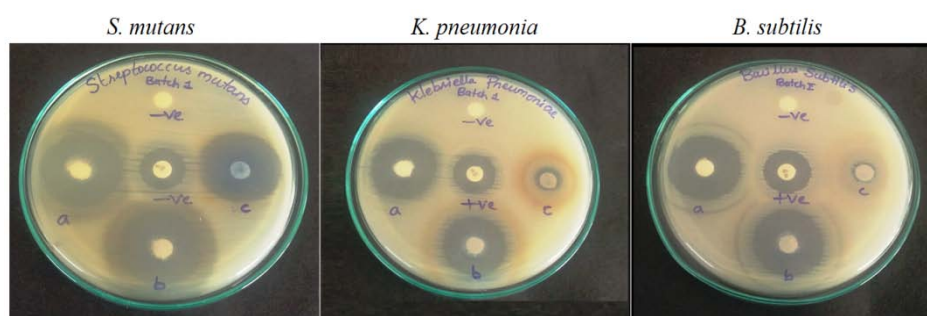


Fig. 7: Images showing the zone of inhibition induced by a) SAXG-NPs-OFLX, b) SAXG-OFLX, and c) pristine Ag NPs for *s. mutans*, *k. pneumoniae*, and *b. subtilis*

Table 2: Shows the zone of inhibition (mm) of SAXG-NPs-OFLX, SAXG-OFLX, and Ag NPs against microorganisms after a 24 h incubation period

Microbial species	Negative control	Positive control	Inhibition zone (mm)		
			SAXG-NPS-OFLX	SAXG-OFLX	Ag NPs
<i>S. mutans</i>	-	17.18±0.24	24.15±1.63	23.17±0.53	22.92±1.11
<i>K. pneumoniae</i>	-	18.48±0.17	24.33±0.26	20.31±0.18	14.05±0.78
<i>B. subtilis</i>	-	16.12±0.14	26.46±0.87	23.51±0.36	11.49±0.91

(mean±SD; n=3).

#### Antibacterial activity

To demonstrate the antibacterial activity of SAXG-NPs-OFLX, SAXG-OFLX, and Ag NPs, they were examined by using *s. mutans*, *k. pneumoniae*, or *b. subtilis* as models (fig. 7). The test samples exhibit antimicrobial activity against *s. mutans*, *k. pneumoniae*, and *b. subtilis*. From table 2, it was observed that SXG-NPs-OFLX has shown a good inhibition zone than the SAXG-OFLX and Ag NPs, which is due to the presence of Ag NPs along with OFLX in the polymer matrix. Interestingly, pristine Ag-NPs showed better antibacterial activity against all three models.

#### CONCLUSION

In this study, SA/XG/Ag-NPs microbeads were synthesized through a simple ionotropic gelation method. FTIR and XRD were used to

validate the interactions between Ag NPs, SA-XG polymeric matrix, and drugs, as well as the molecular level dispersion of OFLX molecules in microbeads. SEM analysis indicated that the beads were spherical with a rough surface and that their average diameter ranged from 700 to 900  $\mu$ m. According to the TEM investigation, the generated NPs range in size from 20 to 40 nm. The Korsmeyer-Peppas equation was applied to find out the release process of developed microbeads. The results show that the release profiles of microbeads follow the non-fiction mechanism. *In vitro* release studies reveal that the high release rate was found at pH7.4. So, it's thought that the SA/XG/Ag-NPs microbeads could work well as drug delivery vehicles for the controlled release of bioactive agents.

#### FUNDING

Nil

**AUTHORS CONTRIBUTIONS**

All authors have contributed equally.

**CONFLICTS OF INTERESTS**

The authors declare that there was no conflict of interest.

**REFERENCES**

- Krithiga N, Rajalakshmi A, Jayachitra A. Green synthesis of silver nanoparticles using leaf extracts of *clitoria ternatea* and *solanum nigrum* and study of its antibacterial effect against common nosocomial pathogens. *J Nanosci.* 2015;2015:1-8. doi: 10.1155/2015/928204.
- Bayda S, Adeel M, Tuccinardi T, Cordani M, Rizzolio F. The history of nanoscience and nanotechnology: from chemical-physical applications to nanomedicine. *Molecules.* 2019;25(1):112. doi: 10.3390/molecules25010112, PMID 31892180.
- Soares S, Sousa J, Pais A, Vitorino C. Nanomedicine: principles, properties, and regulatory issues. *Front Chem.* 2018;6:360. doi: 10.3389/fchem.2018.00360, PMID 30177965.
- Patra JK, Das G, Fraceto LF, Campos EVR, Rodriguez Torres MDP, Acosta Torres LS. Nano-based drug delivery systems: recent developments and future prospects. *J Nanobiotechnology.* 2018;16(1):71. doi: 10.1186/s12951-018-0392-8, PMID 30231877.
- Kalpana VN, Devi Rajeswari V. A review on green synthesis, biomedical applications, and toxicity studies of ZnO NPs. *Bioinorg Chem Appl.* 2018;2018:3569758. doi: 10.1155/2018/3569758, PMID 30154832.
- Ghosh S, Ahmad R, Zeyaulah M, Khare SK. Microbial nanofactories: synthesis and biomedical applications. *Front Chem.* 2021;9:626834. doi: 10.3389/fchem.2021.626834, PMID 33937188.
- Singhal G, Bhavesh R, Kasariya K, Sharma AR, Singh RP. Biosynthesis of silver nanoparticles using *ocimum sanctum* (Tulsi) leaf extract and screening its antimicrobial activity. *J Nanopart Res.* 2011;13(7):2981-8. doi: 10.1007/s11051-010-0193-y.
- Varghese Alex K, Tamil Pavai P, Rugmini R, Shiva Prasad M, Kamakshi K, Sekhar KC. Green synthesized Ag nanoparticles for bio-sensing and photocatalytic applications. *ACS Omega.* 2020;5(22):13123-9. doi: 10.1021/acsomega.0c01136, PMID 32548498.
- Ibrahim N, Jamaluddin ND, Tan LL, Mohd Yusof NY. A review on the development of gold and silver nanoparticles-based biosensor as a detection strategy of emerging and pathogenic RNA virus. *Sensors (Basel).* 2021;21(15):5114. doi: 10.3390/s21155114, PMID 34372350.
- Loiseau A, Asila V, Boitel Aullen G, Lam M, Salmain M, Boujday S. Silver-based plasmonic nanoparticles for and their use in biosensing. *Biosensors.* 2019;9(2):78. doi: 10.3390/bios9020078, PMID 31185689.
- Zhang XF, Liu ZG, Shen W, Gurunathan S. Silver nanoparticles: synthesis, characterization, properties, applications, and therapeutic approaches. *Int J Mol Sci.* 2016;17(9):1534. doi: 10.3390/ijms17091534, PMID 27649147.
- Bruna T, Maldonado Bravo F, Jara P, Caro N. Silver nanoparticles and their antibacterial applications. *Int J Mol Sci.* 2021;22(13):7202. doi: 10.3390/ijms22137202, PMID 34281254.
- Marambio Jones C, Hoek EMV. A review of the antibacterial effects of silver nanomaterials and potential implications for human health and the environment. *J Nanopart Res.* 2010;12(5):1531-51. doi: 10.1007/s11051-010-9900-y.
- Farooqui MA, Chauhan PS, Krishnamoorthy P, Shaik J. Extraction of silver nanoparticles from the leaf extracts of *clerodendrum inerme*. *Dig J Nanomater Biostructures.* 2010;5(1):43-9.
- Paladini F, Pollini M. Antimicrobial silver nanoparticles for wound healing application: progress and future trends. *Materials (Basel).* 2019;12(16):2540. doi: 10.3390/ma12162540, PMID 31404974.
- Yin IX, Zhang J, Zhao IS, Mei ML, Li Q, Chu CH. The antibacterial mechanism of silver nanoparticles and its application in dentistry. *Int J Nanomedicine.* 2020;15:2555-62. doi: 10.2147/IJN.S246764, PMID 32368040.
- Liechty WB, Kryscio DR, Slaughter BV, Peppas NA. Polymers for drug delivery systems. *Annu Rev Chem Biomol Eng.* 2010;1:149-73. doi: 10.1146/annurev-chembioeng-073009-100847, PMID 22432577.
- Borandeh S, Van Bochove B, Teotia A, Seppala J. Polymeric drug delivery systems by additive manufacturing. *Adv Drug Deliv Rev.* 2021;173:349-73. doi: 10.1016/j.addr.2021.03.022, PMID 33831477.
- Obireddy SR, Chintla M, Kashayi CR, Venkata KRKS, Subbarao SMC. Gelatin-coated dual cross-linked sodium alginate/magnetite nanoparticle microbeads for controlled release of doxorubicin. *Chemistry Select.* 2020;5(33):10276-84. doi: 10.1002/slct.202002604.
- Sreekanth Reddy O, Subha MCS, Jithendra T, Madhavi C, Chowdoji Rao K. Curcumin encapsulated dual cross-linked sodium alginate/montmorillonite polymeric composite beads for controlled drug delivery. *J Pharm Anal.* 2021;11(2):191-9. doi: 10.1016/j.jppha.2020.07.002, PMID 34012695.
- Reddy OS, Subha MCS, Jithendra T, Madhavi C, Rao KC. Fabrication and characterization of smart karaya gum/sodium alginate semi-IPN microbeads for controlled release of d-penicillamine drug. *Polym Polym Compos.* 2021;29(3):163-75. doi: 10.1177/0967391120904477.
- Lanjhiyana SK, Bajpayee P, Kesavan K, Lanjhiyana S, Muthu MS. Chitosan-sodium alginate blended polyelectrolyte complexes as potential multiparticulate carrier system: colon-targeted delivery and gamma scintigraphic imaging. *Expert Opin Drug Deliv.* 2013;10(1):5-15. doi: 10.1517/17425247.2013.734805, PMID 23106236.
- Biswas A, Mondal S, Das SK, Bose A, Thomas S, Ghosal K. Development and characterization of natural product derived macromolecules based interpenetrating polymer network for therapeutic drug targeting. *ACS Omega.* 2021;6(43):28699-709. doi: 10.1021/acsomega.1c03363, PMID 34746564.
- Reddy OS, Subha MCS, Jithendra T, Madhavi C, Rao KC, Mallikarjuna B. Sodium alginate/gelatin microbeads-intercalated with kaolin nanoclay for emerging drug delivery in Wilson's disease. *Int J App Pharm.* 2019;11:71-80. doi: 10.22159/ijap.2019v11i5.34254.
- Kuppuswami GM. Fermentation (Industrial), production of xanthan gum. In: Batt CA, Tortorello ML, editors. *Encyclopedia of food microbiology.* 2<sup>nd</sup> ed. Cambridge: Academic Press; 2014. p. 816-21.
- Jithendra T, Reddy OS, Subha MCS, Madhavi C, Rao KC. Xanthan gum graft copolymer/sodium alginate microbeads coated with chitosan for controlled release of chlorthalidone drug. *Int J Pharm Sci Res.* 2020;11(3):1132-45.
- Kar R, Mohapatra S, Bhanja S, Das D, Barik B. Formulation and in vitro characterization of xanthan gum-based sustained release matrix tablets of isosorbide-5-mononitrate. *Iran J Pharm Res.* 2010;9(1):13-9. PMID 24363701.
- Tao Y, Zhang R, Xu W, Bai Z, Zhou Y, Zhao S. Rheological behavior and microstructure of release-controlled hydrogels based on xanthan gum crosslinked with sodium trimetaphosphate. *Food Hydrocoll.* 2016;52:923-33. doi: 10.1016/j.foodhyd.2015.09.006.
- Marslin G, Revina AM, Khandelwal VKM, Balakumar K, Sheeba CJ, Franklin G. Pegylated ofloxacin nanoparticles render strong antibacterial activity against many clinically important human pathogens. *Colloids Surf B Biointerfaces.* 2015;132:62-70. doi: 10.1016/j.colsurfb.2015.04.050, PMID 26005932.
- Pallerla D, Banoth S, Jyothi S. Fabrication of nano clay intercalated polymeric microbeads for controlled release of curcumin. *Int J App Pharm.* 2021;13(1):206-15. doi: 10.22159/ijap.2021v13i1.39965.
- Chinthla M, Obireddy SR, Areti P, Marata Chinna Subbarao S, Kashayi CR, Rapoli JK. Sodium alginate/locust bean gum-g-methacrylic acid IPN hydrogels for "simvastatin" drug delivery. *J Dispers Sci Technol.* 2020;41(14):2192-202. doi: 10.1080/01932691.2019.1677247.
- Costa P, Sousa Lobo JM. Modeling and comparison of dissolution profiles. *Eur J Pharm Sci.* 2001;13(2):123-33. doi: 10.1016/S0928-0987(01)00095-1, PMID 11297896.

33. Obireddy SR, Lai WF. Preparation and characterization of 2-hydroxyethyl starch microparticles for co-delivery of multiple bioactive agents. *Drug Deliv.* 2021;28(1):1562-8. doi: 10.1080/10717544.2021.1955043, PMID 34286634.
34. Jakinala P, Lingampally N, Hameeda B, Sayyed RZ, Khan MY, Elsayed EA. Silver nanoparticles from insect wing extract: biosynthesis and evaluation for antioxidant and antimicrobial potential. *PLOS ONE.* 2021;16(3):e0241729. doi: 10.1371/journal.pone.0241729. PMID 33735177.
35. Cai Y, Piao X, Gao W, Zhang Z, Nie E, Sun Z. Large-scale and facile synthesis of silver nanoparticles via a microwave method for a conductive pen. *RSC Adv.* 2017;7(54):34041-8. doi: 10.1039/C7RA05125E.